CLM-P778

CLM-P778

UKAEA

Preprint

10kW LASER WELDING OF 13mm PRESSURE VESSEL STEEL USING AUTOMATIC WIRE-FEED

I. J. STARES
R. L. APPS
J. H. P. C. MEGAW
J. SPURRIER

CULHAM LABORATORY
Abingdon Oxfordshire

1986

CLM-P778

10kW LASER WELDING OF 13mm PRESSURE VESSEL STEEL USING AUTOMATIC WIRE-FEED

I.J. Stares*, R.L. Apps+. J.H.P.C. Megaw*, J. Spurrier+

*UKAEA Culham Laboratory, Abingdon, Oxon, OX14 3DB, UK

+School of Industrial Science, Cranfield Institute of Technology, Bedford, MK43 OAL, UK

SUMMARY

Laser welding with automatic wire feed has been investigated on UKAEA Culham Laboratory's 10kW CO_2 laser. Welds were made in 13mm thick pressure vessel steel (BS1501-224-490B) and joint gaps up to 2mm have been filled. Welding speed and gap size have been varied and different welding wire compositions used to alter weld metal chemistry. Charpy impact testing on weld metal indicated that the lowest 27J temperature obtained was -50°C. This was achieved using a molybdenum-bearing wire.

(Paper to be presented at the Int. Conf. on Power Beam Technology, Brighton, 10-12 September, 1986).

MAY 1986

INTRODUCTION

The use of filler in laser and electron beam welding is now recognized (1)(2)(3) to offer potential for control of weld metal composition and to relax fit-up considerations. Work at Culham Laboratory has included the use of wire feed with a 5kW CO_2 laser in 6mm thick structural steel (BS4360 Gr 43A) with poorly fitting cropped edges. Structural steel (BS4360 Gr50D) of 8mm thickness was successfully laser welded with a 2mm wide joint gap, and the relationship between weld microstructure and Charpy impact performance was discussed (2)(4). On thicker sections (>10mm) single pass laser welding with wire feed has been achieved (5)(6) with a 10kW CO_2 laser, but published information on weld microstructure and toughness properties is limited.

In general, good toughness properties of autogeneous laser welds have been difficult to achieve in C-Mn and low-alloy steels (2)(7). This seems to be associated with the formation of microstructures of ferrite with aligned martensite-austenite-carbide (MAC) (8). On the other hand, in arc-based welding processes, nucleation of acicular ferrite is known to provide a microstructure with high resistance to cleavage fracture (9); thus use of a suitable filler with laser welding may provide a means of obtaining this structure. In fact, improved impact performance has been reported (10) on 12mm thick HY steel using a Ni alloy shim where the weld microstructures consisted of martensite and bainite.

The objective of the present programme was to investigate welding conditions and different wire filler compositions and their effect on weld microstructure. Charpy impact data is given for: laser welds with no gap (autogeneous); varying joint gap sizes (wire filler composition constant); different wire filler compositions. The heat affected zone properties were not investigated.

EXPERIMENTAL PROGRAMME

Figure 1 shows Culham's 10kW laser installation. The laser (11) is a transverse flow, DC electrically excited device. The output beam leaves the laser via an aerodynamic window, passes through a collimator and propagates 10 metres to a remote workstation. The laser beam, of diameter approximately 40mm, is then focused downwards by a metal mirror f/8 optics system, all the work being carried out with the focus position at the surface of the workpiece. The sample plates, each 500mm x 200mm x 13mm, could be clamped horizontally in pairs to a traversing table to permit a weld length of 500mm. Standard Culham gas shrouding (Fig. 2) was used to provide helium control of the plasma plume above the workpiece and helium shrouding of the upper and lower beads. A fume extractor was placed near the beam/material interaction point to remove welding fumes, which if left, would result in a loss of weld penetration. The wire feeder unit was a commercially-available device with the capability of handling filler wires of diameter 0.9mm, 1.2mm and 1.6mm.

The plate used was a fully-killed aluminium treated C-Mn steel, BS1501-224-490B. A product analysis is given in Table 1. The specification minimum yield strength was $365N/mm^2$ and minimum tensile strength was $509N/mm^2$. The material was received in a normalized condition, hardness 170 HV5, and the microstructure was banded ferrite/pearlite with a grain size of approximately $10\mu m$; the Charpy impact requirements for 41J and 27J temperatures were -30°C and -50°C respectively.

Three of the four MIG arc welding wires used were Cu-coated 1.6mm diameter corresponding to BS2901:Part 1 types A18, A15 and A31. As Table 1 shows, the A18 is a standard double-deoxidised composition; A15 is a triple-deoxidised composition with Ti, Zr and Al additions and A31 is a molybdenum-bearing wire. The fourth welding wire was a nickel alloy wire which had a 1.2mm diameter and complied with the specification AWS A5.28 ER80S-Ni2.

Table 1

Plate and Wire Composition (wt%)

Material	C	Mn	Si	P	S	Mo	Ni	Al	Ti	Zr	Others
Plate BS1501 -224-490B (analysis)	0.16	1.45	0.23	0.021	0.013	0.007	0.03	0.035	-	-	Cr 0.026 Cu 0.04 N 0.006 Sn 0.004 V 0.001
Wire BS2901 Part 1: A18 (specification)	0.12max	0.9/1.6	0.7/1.2	0.04	0.04	-	-	-	-	-	
Wire BS2901 Part 2: A15 (specification)	0.12max	0.9/1.6	0.3/0.9	0.04	0.04	-	-	0.04/0.4	0.15max	0.15max	
Wire BS2901 Part 2: A31 (specification)	0.14max	1.6/2.1	0.5/0.9	0.03	0.03	0.4/0.6	-	-	-	-	
Wire AWS A5.28 ER80S-Ni2 (specification)	0.12max	0.9/1.25	0.4/0.8	0.025	0.025	-	2.5/2.8	-	-	-	

Immediately prior to welding, the machined edges were cleaned with propan-2-ol; joint gaps were made by placing shims at the end of the plates. Welding was carried out in most cases with 9kW at the work. Experiments were arranged in three groups. First, three autogeneous welds were made at 7mms^{-1}, 10mms^{-1} and 14mms^{-1}. Second, keeping fixed the wire composition (A18) and the welding speed (7mms^{-1}), welds were optimised for gap sizes 0.5, 1 and 2mm. Finally, welding conditions were kept constant (10mms^{-1} and ~0.8mm gap) but different welding wires were used.

The welds were subsequently assessed by visual inspection, dye penetrant test, metallography, hardness measurements (values quoted are an average of three readings) and by Charpy tests on full size specimens machined from the plates.

EXPERIMENTAL RESULTS

Wire Feed Technique

The wire feed technique used was substantially as described previously (1) and is shown in Fig. 2. The wire guide nozzle holder was positioned to deliver the wire at approximately 45° to the plate surface and in the same direction as the workpiece movement. For gaps larger than the wire diameter, it was possible to direct the wire so that it was guided by the sidewalls before fusion took place.

The wire feed rate (WFR) was calculated from the welding speed, area of gap to be filled and the cross-sectional area of filler wire. Slight adjustments to the calculated WFR were sometimes necessary in order to obtain good weld appearance; however it was generally found that if the WFR was lower than calculated, underfill would occur and if the WFR was significantly higher than calculated, a weld with a large top bead and poor penetration would result.

For the largest gap of 2mm, particular care was required. With 9kW, the highest practicable welding speed was $7mms^{-1}$, as shown in Fig. 3. Careful alignment was required to avoid lack of sidewall fusion, and in addition, weld drop-out was sometimes encountered. Joint gaps of 0.5mm and 1mm were normally welded consistently and the welding speed could be increased to $10mms^{-1}$. A weld cross-section at this welding condition is shown in Fig. 4.

Autogeneous Weld Properties

Figures 5(a) and (b) show weld microstructures at welding speeds of $7mms^{-1}$ and $10mms^{-1}$. The weld microstructure at the lower speed shows considerable grain boundary ferrite outlining prior austenite grains. Ferrite with aligned MAC was present but there was also some blocky ferrite together with small amounts of martensite and carbide interphases. The weld hardness was 266 HV5. As the welding speed increased, the weld microstructure became more refined (Fig. 5b). Grain boundary ferrite and blocky ferrite were reduced and the amount of ferrite with aligned MAC and martensite increased. The hardness values were 321 HV5 and 360 HV5 for $10mms^{-1}$ and $14mms^{-1}$ respectively.

The Charpy transition curves are given in Fig. 6. In a few cases, the fracture path deviated either into the HAZ or parent material. Indeed, it was impossible to determine the upper shelf behaviour at $7mms^{-1}$ for this reason. However, a sufficient number of specimens fractured in the weld metal to define the transition region. The 40J and 27J temperatures at $7mms^{-1}$ were approximately 10°C and 0°C respectively. These temperatures decreased to approximately -15°C and -30°C at $10mms^{-1}$, but increased again to -2°C and -25°C at $14mms^{-1}$. Thus, with increasing welding speed, hardness rose monotonically whilst impact properties appeared to first improve and then deteriorate. Other electron beam and laser welding experience suggests that hardness and toughness rise together as the low carbon martensite constituent increases. The discrepancy in the present work may possibly be explained by the observations of fine solidification cracks on the Charpy fracture surfaces of the highest speed welds.

Welds with A18 Wire Filler and Different Joint Gaps

Figure 7 shows the Charpy transition curves for welds carried out with the double-deoxidised wire filler at 9kW, $7mms^{-1}$ and for gaps of 0.5, 1 and 2mm; also shown is the $7mms^{-1}$ autogeneous curve from Fig. 6. It is seen that the 40J and 27J temperatures were approximately -20°C and -35°C for the 0.5mm gap and approximately -10°C and -30°C for the 2mm gap. Both conditions therefore show an improvement over autogeneous welds at $7mms^{-1}$ and are indeed comparable to those at $10mms^{-1}$. The weld hardnesses for the 0.5 and 2mm gaps were 286 and 290 HV5 respectively, somewhat higher than the corresponding $7mms^{-1}$ autogeneous welds. However, they are lower than those for the $10mms^{-1}$ autogeneous welds i.e. comparable impact properties can be achieved at lower hardness. The Charpy curve for the 1mm gap is believed to be anomalously low due to significant lack of side-wall fusion which was observable on the fracture surfaces. Additionally, porosity with typical pore diameter ~1mm was also observed there. It should be noted that porosity was not observed in the 0.5 and 2mm gap cases and it is not clear at present exactly what change in technique caused its appearance.

Figure 8 shows microstructure in the 2mm gap weld. This is representative of the microstructure seen in all three gap cases i.e. there does not appear to be a strong correlation between microstructure and dilution. In contrast to the autogeneous welds, there is now a certain amount of coarse acicular ferrite.

Welds with Different Wire Fillers

Figure 9 shows the Charpy results for welds carried out for the four wires with 9kW, $10mms^{-1}$ and a 0.8mm gap. Porosity was seen, to varying degrees, on the fracture surfaces of all four welds. Porosity levels were highest for the triple-deoxidised wire, were much reduced for the double deoxidised wire and were further decreased for the Mo and Ni wires. At this stage is would be premature to correlate porosity levels with wire type since the results of the previous section showed that the A18 wire type (albeit at a slightly slower welding speed) could produce welds which were either with or without porosity. The curves have been fitted by eye to the data points, which exhibit some scatter. The approximate 40J and 27J temperatures are given in Table 2, together with weld metal hardness.

Table 2 - 40J and 27J temperatures and weld metal hardness (HV5)

Wire Filler	40J	27J	HV5
A18	-10°C	-24°C	332
A15	20°C	0°C	330
A31	-10°C	-50°C	361
Ni	-20°C	-35°C	362

It is seen that: the poorest impact properties occur with the triple-deoxidised wire; matters improved with the double-deoxidised wire; the molybdenum and nickel wires were slightly better still, with the former apparently showing best lower shelf properties (in fact, its 27J temperature of -50°C matches parent plate specification).

Figure 10 shows microstructures of the four welds. Those for the double and triple-deoxidised filler wires (Figs. 10a and b) both show substantial amounts of ferrite with aligned MAC. However the former had a coarser structure (similar to that for the slow autogeneous weld, Fig. 5a) whilst the latter showed a small amount of acicular ferrite. For the A18, it may be noted that a negligible quantity of acicular ferrite was seen here ($10mms^{-1}$ and 0.8mm gap) compared with that seen at $7mms^{-1}$ and 2mm gap (Fig. 8). Figures 10c and d show that the use of molybdenum and nickel filler wires increased the amount of martensite present; a higher level of martensite was seen with the nickel wire, although this is not reflected in the hardness measurements.

CONCLUSIONS

Results have been presented for the 9kW laser welding of BS1501-224-490B steel plate of 13mm thickness: (i) autogeneously at three speeds; (ii) with filler at one speed and three gap sizes; (iii) for one speed and gap size but for four different fillers. Analysis has been confined so far to hardness measurements optical microscopy and Charpy impact testing. Charpy testing of these narrow welds produced some fracture deviation (12), but those results have been disregarded.

Addition of filler is easier for the narrow gaps investigated here, whilst the filling of the 2mm gap required care; indeed, even one of the 1mm gap welds exhibited lack of sidewall fusion. Out of seven full-size plate welds with filler, five contained porosity to varying degrees and two were essentially pore-free. There is no clear correlation between porosity and, say, gap size or wire type; provisionally it is suggested that the effect may be predominantly associated with experimental procedure rather than materials compositions.

The autogeneous welding showed: with increasing speed, weld microstructures which exhibited increasing refinement and martensitic content; that hardness values increased; and that impact performance first improved and then deteriorated somewhat. The deterioration is believed to be associated with the onset of solidification cracking at the highest speed. This emphasises part of the motivation behind adding wire feed to laser welds i.e. filler will hopefully permit avoidance of this cracking which can be prevalent in the fast autogeneous welding of C-Mn steels by electron and laser beams.

The filler welds on different gap sizes (double-deoxidised wire) showed that for a 0.5mm gap the impact performance was comparable to the best autogeneous weld, but the hardness was lower. Increasing the gap to 2mm results in some reduction of impact performance.

The welds with four fillers suggested that the triple deoxidised wire gave worst impact performance, and of the other three the molybdenum wire was probably best. Although molybdenum has been shown in arc welding (13) to improve toughness by reducing grain boundary ferrite and promoting acicular ferrite and an even distribution of martensitic microphases, no significant quantities of acicular ferrite were seen here. Whether this is due to the more rapid thermal cycle, or possibly to a reduction of nucleation sites by evaporation, is not clear at present. In fact, in this programme, best impact properties appear to correlate with increased martensite content. The impact performance of the molybdenum wire was better than the best autogeneous weld, and in particular its 27J temperature of -50°C matches parent plate specification.

ACKNOWLEDGEMENTS

The authors gratefully acknowledge the cooperation of colleagues in the Laser Applications Group at UKAEA Culham Laboratory and in the School of Industrial Science at Cranfield Institute of Technology. At Culham, special mention is made of the interest in the work of Dr IJ Spalding, and of the experimental assistance of Messrs SJ Osbourn and B Hewlett.

REFERENCES

1. Megaw JHPC, Hill M, and Johnson R: 'Laser welding of steel plates with unmachined edges'. Proc Conf Inst of Metallurgists Joining of Metals - Practice and Performance Warwick April 1981.
2. Watson MN and Dawes CJ: 'Laser welding deep drawing steel sheet and microalloyed plate'. Metal Construction 1985 17 (9) 561-565.
3. Kanatani F et al: 'Electron beam welding with filler metal'. 3rd Int Colloq on Welding and Melting by Electron and Laser Beams Lyon 5-9 September 1983.
4. Watson MN: 'Laser welding of structural steels with wire feed'. Weld Inst Res Report 264/1985.
5. Megaw JHPC, Hill M, Nicholson CJ and Stares IJ: 'The use of filler in laser welding' Culham Laboratory Laser Users' Club (Members' Report, 1985).
6. Martyr DR: ' High power laser applications in the shipbuilding industry'. Trans North East Coast Institute of Engineers and Shipbuilders, 1983 99 (3) 106-109.
7. Megaw JHPC, Hill M, and Osbourn SJ: 'Girth welding of X-60 pipeline with a 10kW laser'. Proc Conf High Power Lasers and Their Industrial Applications, Innsbruck, 15-18 April 1986, SPIE Proceedings Vol 650. Also

as Culham preprint CLM-P773.
8. Abson DJ and Dolby RE: ' A scheme for the quantitative description of ferrite weld metal microstructure'. Weld Inst Res Bull 1980 21 (4) 100-103.
9. Dolby RE: 'Advances in welding metallurgy of steels'. Metals Technology 1983 10 349-362.
10. Metzbower EA and Moon DW: 'The effects of Inconel 600 on the toughness of HY steel'. Lasers in Material Processing American Society of Metals, Meta[illegible] Park 1983 248-253.
11. Licensee: Ferranti Industrial Electronics Ltd, Dunsinane Avenue, Dundee, DD2 3PN, UK.
12. Goldak JA and Nguyen DS: 'A fundamental difficulty in Charpy V-notch testing narrow zones in welds'. Welding Journal Research Supplement, 1977 56 (4) 1195s-1254s.
13. Garland JG and Kirkwood PR: 'Towards improved submerged arc weld metal'. Metal Construction May 1975 275-283 June 1975 320-330.

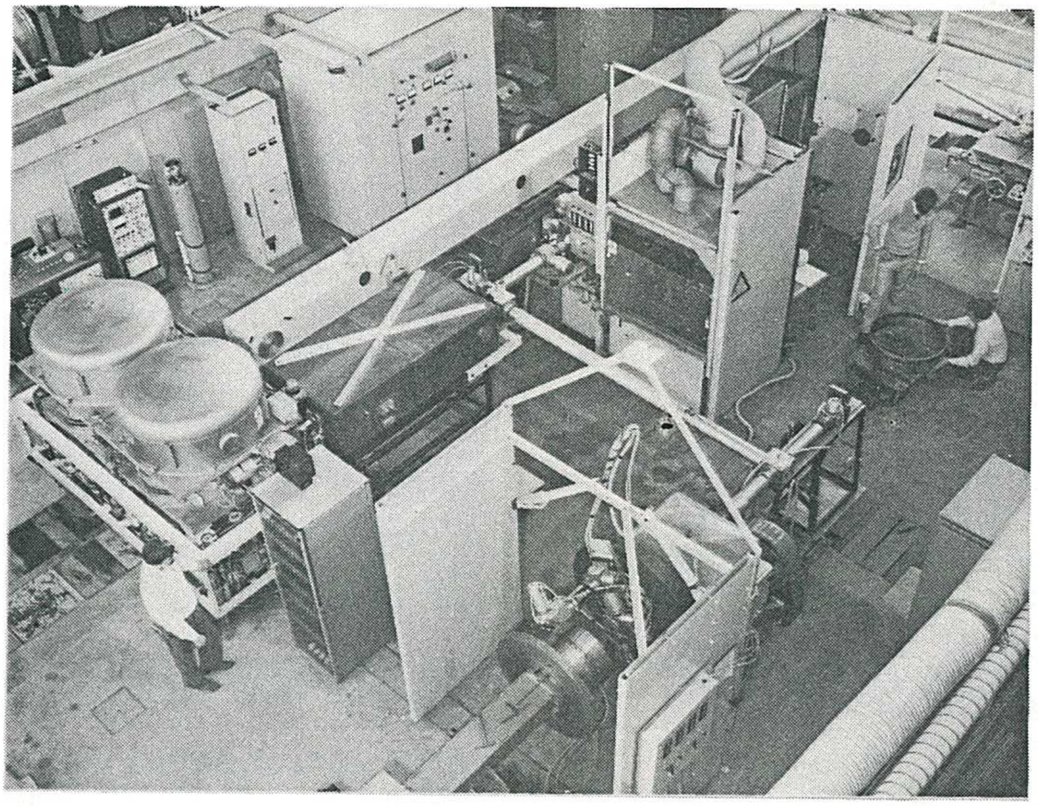

1. CL10 Laser Area

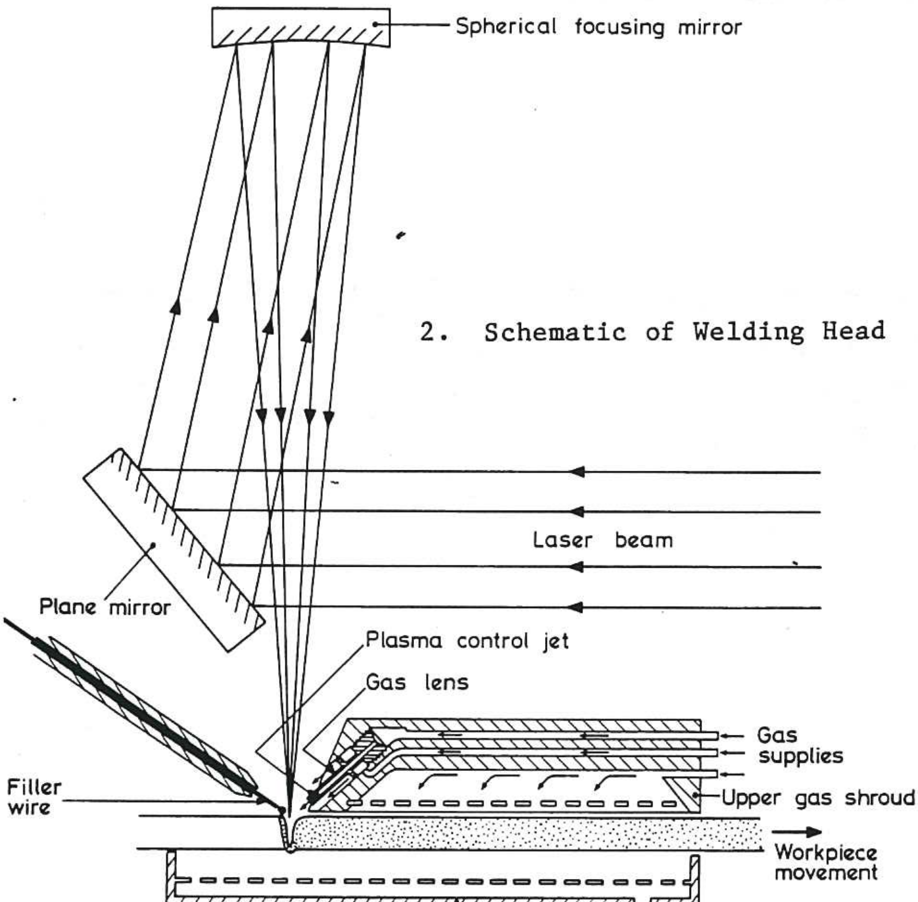

2. Schematic of Welding Head

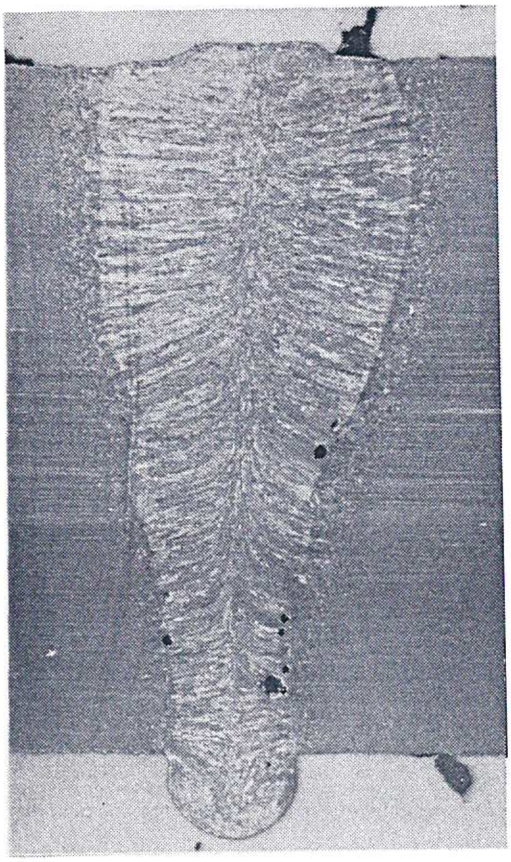

3. Weld profile with filler (x7)
welding condition: 7mms^{-1}; 2mm gap

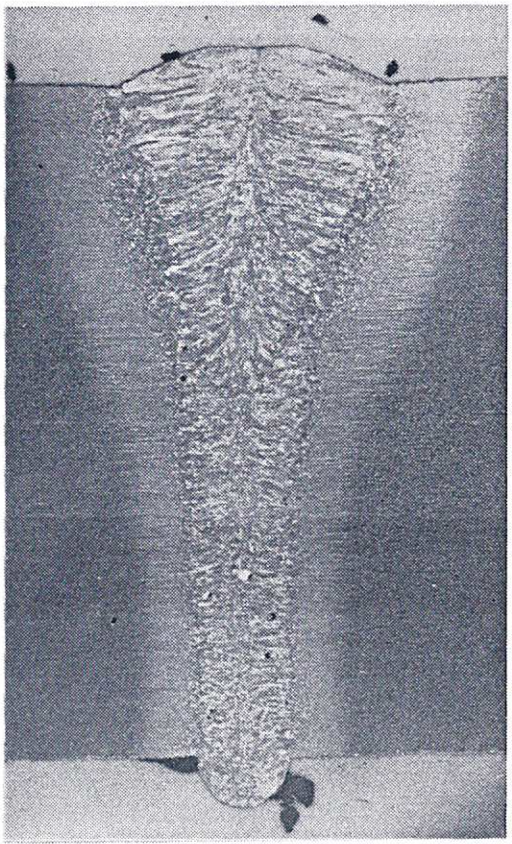

4. Weld profile with filler (x7)
welding condition: 10mms^{-1}; ~0.8mm gap

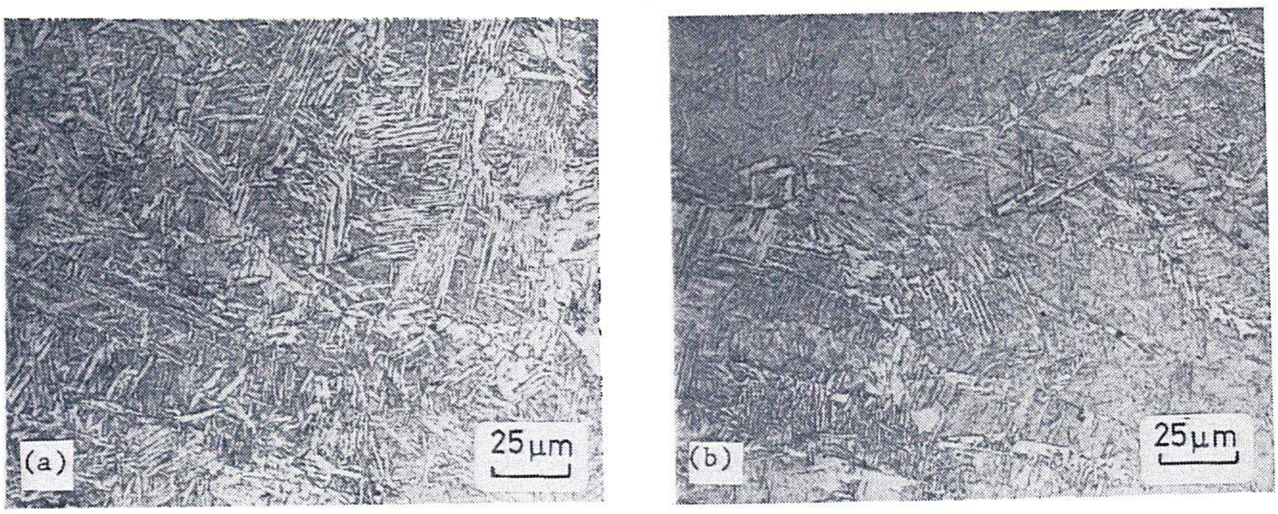

5. Microstructures of autogeneous welds at (a) 7mms^{-1}; (b) 10mms^{-1} (nital etch)

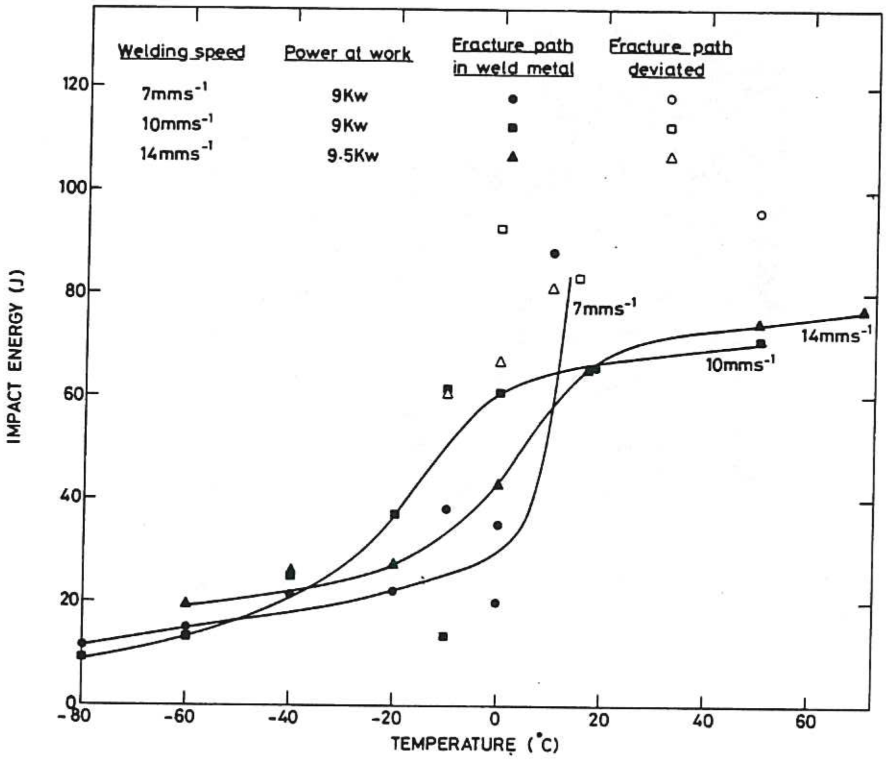

6. Impact transition curves of autogeneous welds.

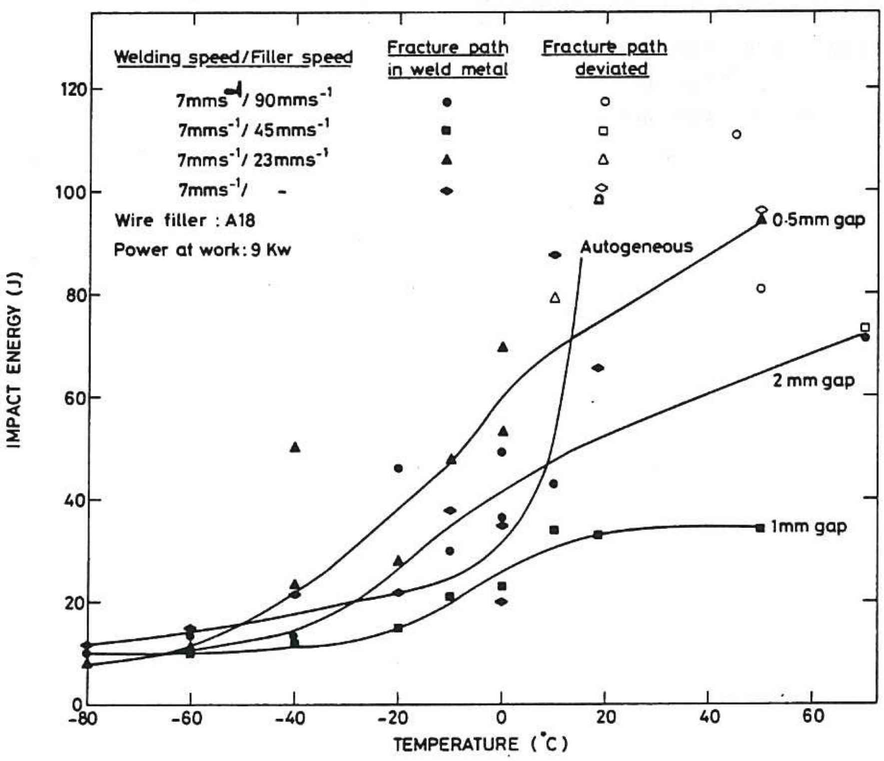

7. Impact transition curves of welds containing wire filler: A18 and varying gap size.

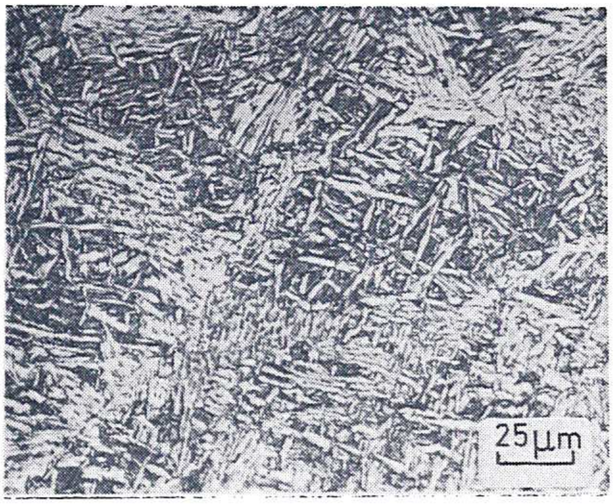

8. Microstructure of weld with 2mm gap containing A18 wire filler (nital etch).

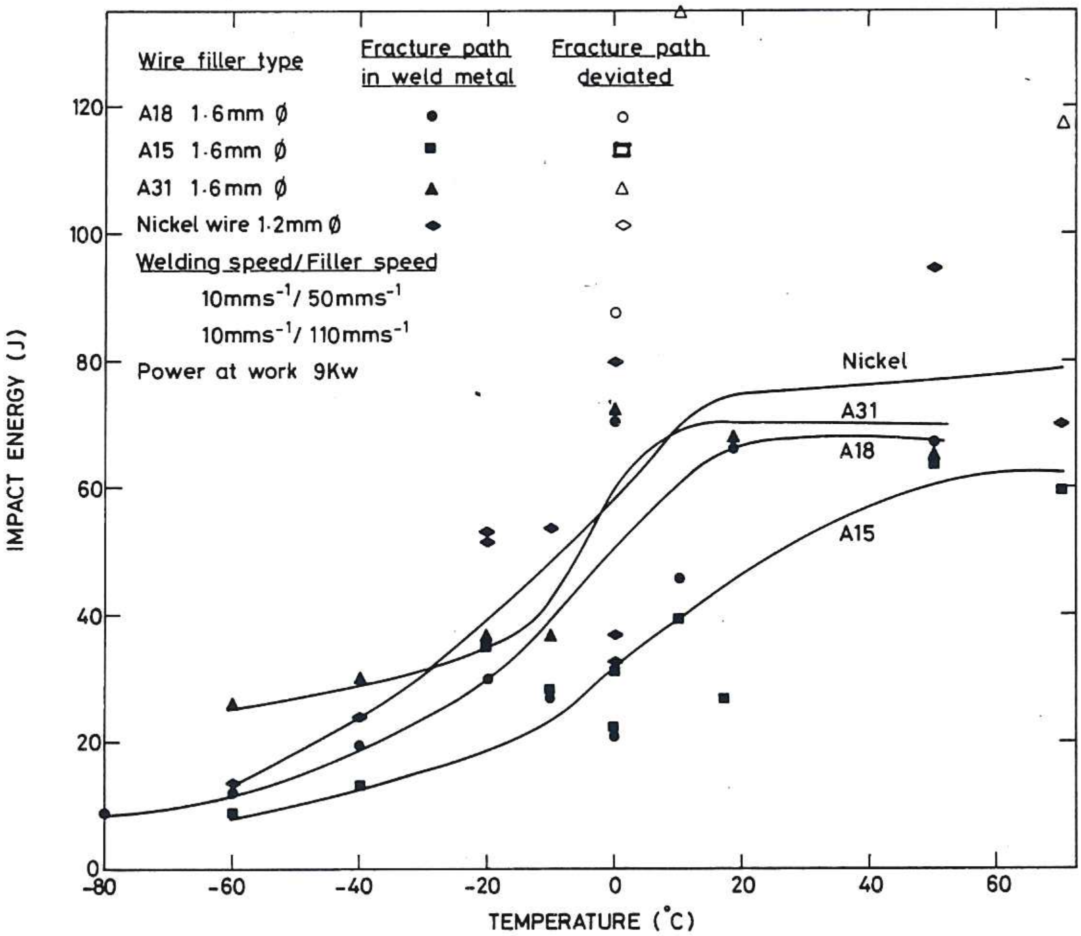

9. Impact transition curves of welds containing wire filler: A18, A15, A31 and Nickel.

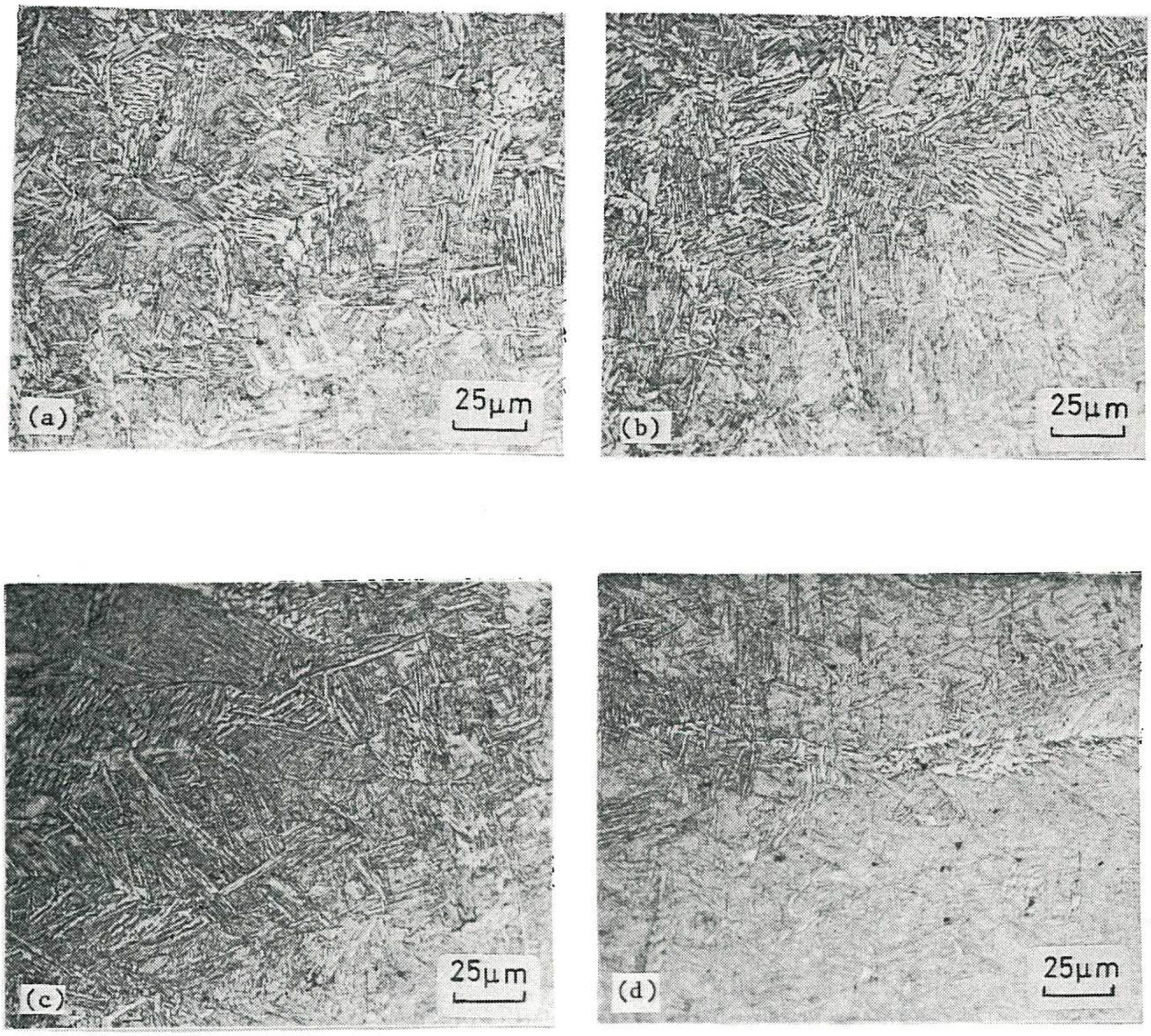

10. Microstructures of laser welds with (a) A18 wire filler; (b) A15 wire filler; (c) A31 wire filler; (d) 2% Ni wire filler (nital etch)